

## AN OBSERVATIONAL ASSESSMENT OF OFF-HODOGRAPH DEVIATIONS FOR USE IN OPERATIONAL SUPERCELL MOTION FORECASTING METHODS

Matthew J. Bunkers\*

NOAA/NWS Weather Forecast Office, Rapid City, South Dakota

### 1. INTRODUCTION

Significant advances have been made in the operational understanding and prediction of supercell motion since the late 1990s (Rasmussen and Blanchard 1998; Bunkers et al. 2000, hereafter B2K; Klimowski and Bunkers 2002; Zeitler and Bunkers 2005). A key consideration has been the deviation–propagation of updrafts to the right of the vertical wind shear for counterclockwise rotating supercells (RM), and to the left of the wind shear for clockwise rotating supercells (LM; Fig. 1). This represents a paradigm shift from the previous conceptual model of viewing the deviate motion of supercells with respect to the vector mean wind—a perspective that produces inconsistent results (e.g., Davies-Jones 2002; Zeitler and Bunkers 2005).

It has been shown that to a first approximation supercell motion is the sum of (1) an *advective component* and (2) a *propagation component* which is dependent upon interactions of the updraft with the vertically sheared environment (e.g., Weisman and Rotunno 2000). This “updraft–shear” propagation is linear for purely circular hodographs and nonlinear for straight hodographs (Davies-Jones 2002). Furthermore, the updraft–shear interactions can produce 40–60% of the total updraft strength (Weisman and Klemp 1984; Weisman and Rotunno 2000); hence these interactions are a very important determinant of supercell motion (e.g., Fig. 1).

Observationally based supercell motion forecasting methods (Rasmussen and Blanchard 1998; B2K) which have capitalized on the above information implicitly assumed this shear-induced off-hodograph deviation,  $D$ , to be fixed (i.e.,  $8.6 \text{ m s}^{-1}$  or  $7.5 \text{ m s}^{-1}$ , respectively). This does not necessarily mean  $D$  should be constant; much variability in  $D$  was noted by B2K and Ramsay and Doswell (2005). However, the choice of a constant  $D$  was based on the minimization of the mean forecast motion error for all supercells in the samples.

Several modeling studies suggest  $D$  is in part a function of the strength of the vertical wind shear (e.g., Weisman and Klemp 1984; Droegemeier et al. 1993; Weisman and Rotunno 2000), as well as other thermodynamic variables such as CAPE, LCL, and precipitable water (Kirkpatrick et al. 2006). These modeling studies contend that  $D$  increases as the

vertical wind shear increases—especially in the lowest 3–6 km of the troposphere. Based on earlier simulations, Lilly (1982) noted that storms moving laterally to rectilinear shear do so at a slower rate than they do for a rotating mean hodograph with the same buoyancy (i.e., the greater the hodograph curvature the greater the off-hodograph deviation). Moreover, for the case of linear propagation, the magnitude of  $D$  may depend upon the updraft width, with wide updrafts deviating farther off the hodograph than narrow updrafts (Davies-Jones 2002).

Information from the above studies may be useful in contriving an adaptable (or dynamic)  $D$  that potentially could reduce the errors in supercell motion forecasts. Thus, the variability of this off-hodograph deviation,  $D$ , will be studied herein using a database of 425 observed soundings and supercells. The goal is to determine the feasibility of deriving a flexible  $D$  for supercell motion forecasting methods.

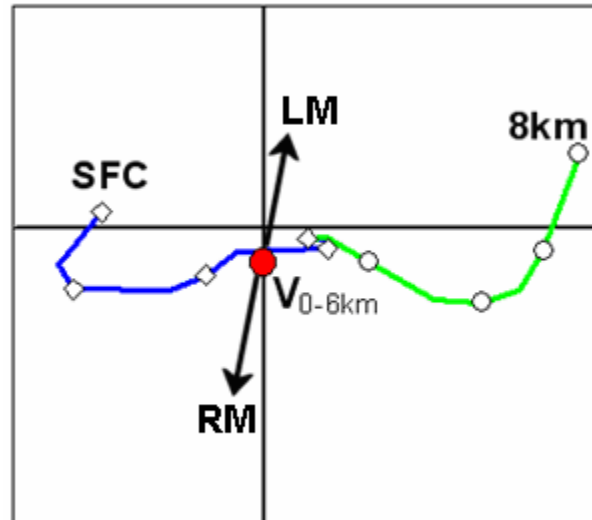


**Figure 1.** Hodograph derived from the 0-h RUC for Lamar, CO, valid 2300 UTC 22 July 2004. Vectors represent the off-hodograph deviation,  $D$ , for right-moving (RM) and left-moving (LM) supercells. The red circle denotes the mean wind. Data are plotted every 500 m but are marked every 1000 m.

### 2. DATA AND METHODS

#### 2.1 Dataset

The 425 observed soundings and supercells were obtained using standard methods. Soundings were representative of the inflow region of the supercells, and supercells generally occurred within 3 h and 185

\* Corresponding author address: Dr. Matthew J. Bunkers, National Weather Service, 300 E. Signal Dr., Rapid City, SD 57701-3800; e-mail: [matthew.bunkers@noaa.gov](mailto:matthew.bunkers@noaa.gov).

km (100 n mi) of the sounding release point. Ninety-two percent of the cases were associated with a 0000 UTC release. The observed supercell motion was calculated during the steadiest part of the supercell using a period of around 60 min. Furthermore, each case consists of a single unmodified sounding so as to avoid problems associated with smoothing and subjective modifications.

## 2.2 Computing Off-Hodograph Deviation (D)

The off-hodograph deviation,  $D$ , is defined as the shear-orthogonal distance from the mean wind to the observed supercell motion. Starting with an unmodified hodograph (e.g., Fig. 2a),  $D$  was computed as follows:

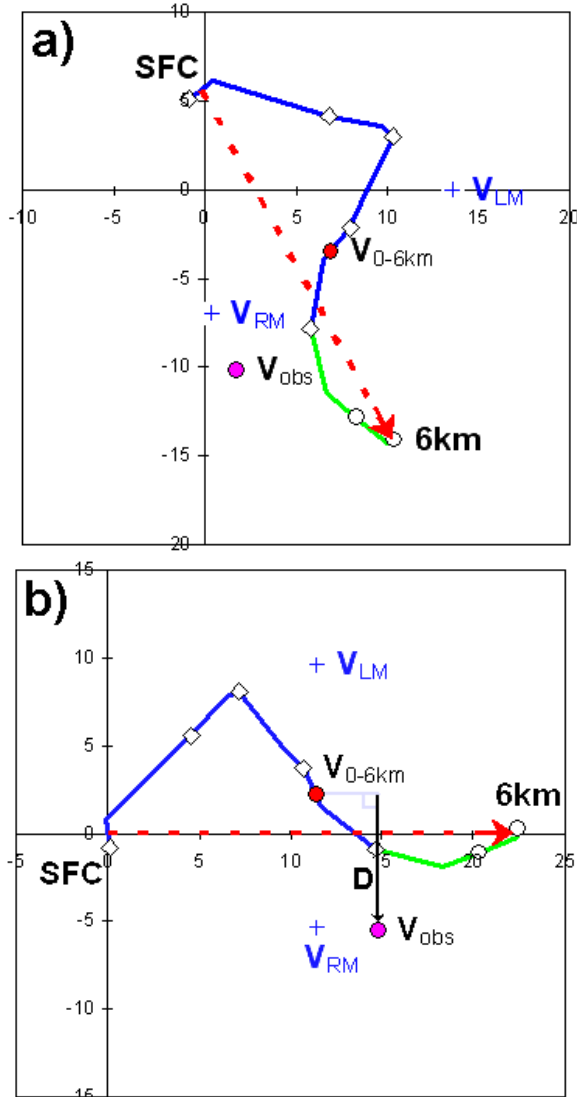


**Figure 2.** (a) Hodograph for Norman, OK, valid 0000 UTC 29 July 2000. (b) Same as a) except that it has been translated as described in the text. The red (purple) circles denote the mean wind (observed motion). The dashed red vectors denote the shear vector from 0–0.5 to 5.5–6 km, and the black vector in b) represents  $D$ . Predicted supercell motions are  $V_{RM}$  and  $V_{LM}$ .

- The hodograph was translated such that (i) the shear vector from 0–0.5 to 5.5–6 km (red dashed arrow in Fig. 2) was aligned with the  $x$ -axis and (ii) the 0–0.5-km mean wind was at the origin (Fig. 2b).
- Next,  $D$  was calculated by taking the difference between the translated  $v$ -components of the 0–6-km mean wind ( $V_{0-6km}$ ) and the observed supercell motion ( $V_{obs}$ ). For example,  $D = 7.5 \text{ m s}^{-1}$  in Fig. 2b (refer to the black vector).

Note that  $D$  is not simply the deviation of  $V_{obs}$  from  $V_{0-6km}$  (e.g.,  $8.4 \text{ m s}^{-1}$  in Fig. 2; also see B2K and Ramsay and Doswell 2005), nor is  $D$  the distance from  $V_{obs}$  to the nearest point on the hodograph (e.g.,  $4.6 \text{ m s}^{-1}$  in Fig. 2). Therefore, by this definition, a supercell with a motion that is  $5 \text{ m s}^{-1}$  transverse to a unidirectional hodograph *could* have a larger  $D$  than a supercell with a motion that is near the center of a circular hodograph (and where the deviation from the mean wind is  $< 5 \text{ m s}^{-1}$ ). The average observed  $D$  for all 425 cases is  $7.7 \text{ m s}^{-1}$ .

## 2.3 Determining the Potential Improvement in D

The potential improvement in predicted supercell motion was determined by applying the B2K method to each case using the observed  $D$  from above (versus a fixed  $D$ ). The mean vector error (MVE) was  $2.09 \text{ m s}^{-1}$  for this procedure. Next, the B2K method was run with  $D$  fixed at  $7.5 \text{ m s}^{-1}$  for each of the 425 cases, and the MVE increased to  $3.09 \text{ m s}^{-1}$ . This suggests the MVE could be reduced by as much as  $1.0 \text{ m s}^{-1}$  assuming the perfect scenario where the optimal  $D$  could be prescribed beforehand.

## 2.4 Comparison of $D$ with Sounding Variables

Based on the literature cited in section 1, several sounding variables were correlated with  $D$  (Table 1). In addition, a variety of ratios (e.g.,  $MLCAPE_{3km}/MLCAPE$ ,  $Bulk_{0-1km}/Bulk_{0-6km}$ ) was examined to see if the distribution of buoyancy and/or shear was of importance. Thermodynamic variables were derived using a mean-layer (ML) parcel over the lowest 1000 m and the virtual temperature correction. The storm-relative helicity (SRH) was calculated using the predicted supercell motion of B2K since the observed

|                        |                          |                          |
|------------------------|--------------------------|--------------------------|
| SRH <sub>3km</sub>     | MLCIN                    | MLLCL                    |
| MLVGP                  | MLCAPE                   | MLLFC                    |
| MLEHI                  | MLCAPE <sub>3km</sub>    | MLEL                     |
| Bulk <sub>0-xkm</sub>  | MLCAPE <sub>500hPa</sub> | PW <sub>sfc-300hPa</sub> |
| Total <sub>0-xkm</sub> | LR <sub>850-700hPa</sub> |                          |

**Table 1.** Sounding variables used for the correlation analysis with  $D$ . For Bulk<sub>0-xkm</sub> and Total<sub>0-xkm</sub> the upper level was varied from  $x = 1$  to 8 km. Refer to section 2.4 for a discussion of these variables.

supercell motion is not known in an operational setting before storms develop. Moreover, the goal of this research is to be able to better predict the observed supercell motion, thus it cannot be a predictor itself. The scalar difference in the wind between two different levels ( $Bulk_{0-xkm}$ ) and the summation of the hodograph segments between two different levels ( $Total_{0-xkm}$ ) were used to gauge the vertical wind shear.

### 3. RESULTS

#### 3.1 Kinematic Variables

In general the correlation coefficients between D and the proxies for wind shear were similar for the layers 0–2 km through 0–8 km (Fig. 3). The coefficients averaged 0.07 larger for  $Total_{0-xkm}$  versus  $Bulk_{0-xkm}$ , but there was no well-defined peak in either distribution. The values of around 0.25 for  $Total_{0-xkm}$  are generally supportive of the modeling studies cited in section 1. The correlation coefficient between D and  $SRH_{3km}$  was also relatively large (0.26, very near the values for  $Total_{0-xkm}$  in Fig. 3). Although the differences between these coefficients and zero are statistically significant, they only explain 3–8% of the variance and are thus “practically” insignificant according to Livezey (1999).

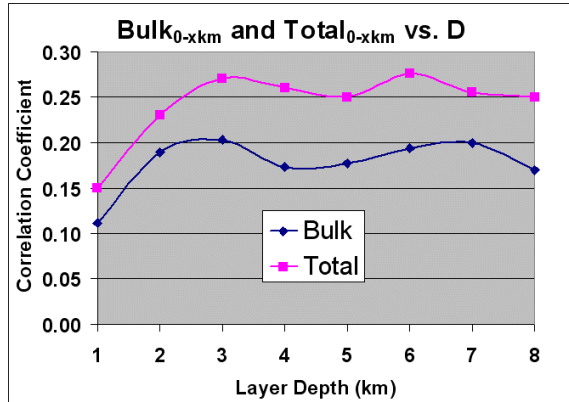


**Figure 3.** Correlation coefficients between D and the shear-related variables,  $Bulk_{0-xkm}$  and  $Total_{0-xkm}$ . The layer depth is represented by x in  $Bulk_{0-xkm}$  and  $Total_{0-xkm}$ .

As noted in section 2.4, the distribution of shear was also examined. This was done in order to assess the relative contributions of compressed shear (e.g., relatively large  $Bulk_{0-3km}/Bulk_{0-6km}$ ) and distributed shear (e.g.,  $Bulk_{0-3km}/Bulk_{0-6km}$  near 0.5). The largest of these correlation coefficients was only 0.10 for the ratios  $Total_{0-2km}/Total_{0-8km}$  and  $Total_{0-3km}/Total_{0-8km}$ , indicating a very slight tendency for larger D as the shear is compressed in the lower part of the troposphere [as in Kirkpatrick et al. (2006)]. Nevertheless, the smallness of the coefficients reflects a rather poor observational relationship between the shear distribution and the off-hodograph deviation, D.

#### 3.2 Thermodynamic Variables

The correlation coefficients for the thermodynamic variables were even smaller than those for the kinematic variables (Table 2). MLCAPE produced the largest coefficient (0.10), which suggests a very slight tendency for larger D as the buoyancy increases (i.e., greater off-hodograph propagation as updraft strength increases). Interestingly, the trend is opposite as buoyancy is compressed in the lower part of the troposphere (i.e., smaller D as the percentage of buoyancy increases below 3 km/500 hPa). Again, the smallness of these correlation coefficients means that the thermodynamic variables do not appear useful in improving D for supercell motion forecasting methods. This is difficult to reconcile with the modeling study of Kirkpatrick et al. (2006) in which thermodynamics were found to have a notable influence on supercell motion.

|   |  |
|---|--|
| MLCAPE ( $r = 0.10$ )                   | MLLCL ( $r = -0.05$ )                    |
| MLCAPE <sub>3km</sub> ( $r = 0.02$ )    | MLLFC ( $r = -0.01$ )                    |
| MLCAPE <sub>500hPa</sub> ( $r = 0.07$ ) | MLEL ( $r = 0.09$ )                      |
| %CAPE < 3 km ( $r = -0.09$ )            | PW <sub>sfc-300hPa</sub> ( $r = 0.02$ )  |
| %CAPE < 500 hPa ( $r = -0.09$ )         | LR <sub>850-700hPa</sub> ( $r = -0.06$ ) |
| MLCIN ( $r = 0.03$ )                    |  |

**Table 2.** Correlation coefficients between D and the thermodynamic-related variables.

#### 3.3 Kinematic–Thermodynamic Combinations

The results of the correlation analysis did not improve after combining the thermodynamic and kinematic information. For example, the correlation coefficient between D and the ML vorticity generation parameter (MLVGP, Rasmussen and Blanchard 1998) was 0.24 (Fig. 4)—similar to those for  $Total_{0-xkm}$ . Furthermore, the coefficient was 0.24 for the ML energy-helicity index (MLEHI; Hart and Korotky 1991). Also note the scatter plot in Fig. 4 is characteristic of

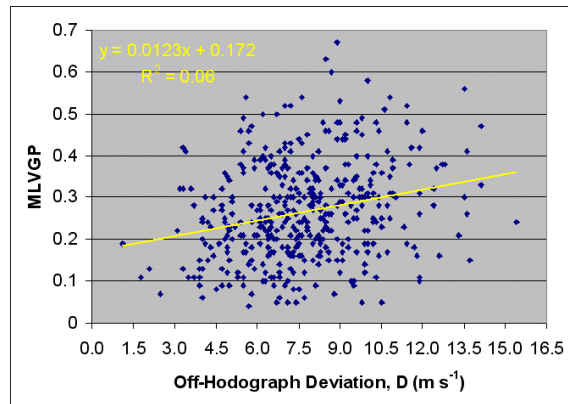


**Figure 4.** Scatter plot of D versus MLVGP for 425 observations. The yellow line is the least squares fit to the data, and the corresponding linear regression equation is given in the upper-left part of the figure.

those for the kinematic variables discussed in section 3.1. From this it is apparent that a single variable is potentially as useful as a combination of variables.

### 3.4 Potential Modifications to the B2K Method

The previous results suggest that if the B2K method is to be improved, D should be based on one of the following: Total<sub>0-3km</sub>, Total<sub>0-6km</sub>, SRH<sub>3km</sub>, MLVGP, or MLEHI. Each of these variables was therefore used in a simple linear regression model to arrive at  $D = mx + b$  where  $x$  is one of the five variables.

These variants of D resulted in only a minimal improvement in the MVEs (Table 3). For reference, the baseline B2K method produced an MVE of  $3.09 \text{ m s}^{-1}$  for the 425 cases. The largest improvement was derived from Total<sub>0-6km</sub>, which helped reduce the MVE by  $0.07 \text{ m s}^{-1}$  (i.e., from  $3.09$  to  $3.02 \text{ m s}^{-1}$ ). Considering the potential improvement in D (refer to section 2.3), this reduction represents 7% of the total. Recall that  $r = 0.28$  between D and Total<sub>0-6km</sub> (Fig. 3), which yields an  $r^2 = 7.8\%$ . From an operational forecasting perspective, this improvement is meteorologically insignificant. For completeness the MLCAPE was also tested, and the MVE was  $3.08 \text{ m s}^{-1}$  (nearly identical to the MVE for the B2K method using  $D = 7.5 \text{ m s}^{-1}$ ).

| Variable used to modify D | Mean Vector Error ( $\text{m s}^{-1}$ ) |
|---------------------------|---|
| Total <sub>0-3km</sub>    | 3.03                                    |
| Total <sub>0-6km</sub>    | 3.02                                    |
| SRH <sub>3km</sub>        | 3.03                                    |
| MLVGP                     | 3.04                                    |
| MLEHI                     | 3.05                                    |

**Table 3.** MVEs for the B2K method using a variable D as discussed in section 3.4. For comparison purposes, the baseline B2K method with  $D = 7.5 \text{ m s}^{-1}$  produced an  $MVE = 3.09 \text{ m s}^{-1}$ .

### 3.5 Downshear Deviations

Although not a specific focus of this study, the downshear deviations in supercell motion were also briefly examined. Referring to Fig. 2b, this deviation is defined as the shear-parallel distance from the mean wind to the observed supercell motion (i.e., the difference in the  $u$ -components represented by the light purple line).

Those variables possessing the largest correlation coefficients with the downshear deviations are given in Table 4. Now the thermodynamic variables display a much larger signal (compared to section 3.2), with a propensity for downshear deviation as the LCL/LFC heights are raised and as the MLCAPE is relatively minimized in the lowest 3km AGL. This is suggestive of storms that are outflow dominated (e.g., many HP supercells may fit this genre), and may help explain some of the differences between the present study and that of Kirkpatrick et al. (2006). Also of note is the

modest tendency for *increasing* downshear deviations as the low-level shear *decreases*, and vice versa.

|                                       |   |
|---------------------------------------|---|
| MLCAPE <sub>3km</sub> ( $r = -0.31$ ) | Bulk <sub>0-1km</sub> ( $r = -0.27$ )                           |
| %CAPE < 3 km ( $r = -0.26$ )          | Bulk <sub>0-2km</sub> ( $r = -0.24$ )                           |
| MLLCL ( $r = 0.26$ )                  | Total <sub>0-1km</sub> ( $r = -0.24$ )                          |
| MLLFC ( $r = 0.24$ )                  | Bulk <sub>0-1km</sub> / Bulk <sub>0-6km</sub> ( $r = -0.22$ )   |
|                                       | Total <sub>0-1km</sub> / Total <sub>0-6km</sub> ( $r = -0.27$ ) |

**Table 4.** Correlation coefficients between the downshear deviations and select sounding variables.

## 4. SUMMARY AND CONCLUSIONS

The results of the correlation analysis suggest there may be a real connection between the vertical wind shear and the off-hodograph deviation, D, which is well supported by previous modeling studies. Unfortunately, the relationship does not appear strong enough to sufficiently improve D for supercell motion forecasting methods. The thermodynamic variables offered even less hope for improving the D parameter (although there is a signal for downshear deviations), despite the promising modeling results of Kirkpatrick et al. (2006). Therefore, in the short term it will remain difficult to improve error statistics below  $2-3 \text{ m s}^{-1}$  for supercell motion forecast methods, and thus a fixed D is still on par with a “dynamic” D.

Why is it seemingly so difficult to improve upon the D parameter? First, there are several other propagation mechanisms that affect supercell motion (Zeitler and Bunkers 2005). For example, mesoscale boundaries and storm-scale interactions are not represented in the sounding database, but they sometimes have profound effects on supercell motion. This could be masking the signal in the present study. Second, the relationship between D and sounding variables may be nonlinear. The present study only examined simple linear relationships. Last, the influence of updraft width upon deviate motion was not investigated herein, and this could be further masking any meaningful signal.

In closing, it may be that going up another level in complexity from hodograph-based techniques is going to entail considerable effort, and it is estimated that even a full-blown numerical model will not substantially reduce the MVE below  $2 \text{ m s}^{-1}$ . Thus, operationally it seems that minimal additional benefit is gained for the time investment to modify the off-hodograph deviation used in forecasting supercell motion.

## 5. ACKNOWLEDGEMENTS

I would like to thank Dan Miller and Jon Zeitler for reviewing this paper and providing valuable input for its improvement. I also appreciate the reference information provided by Cody Kirkpatrick as well as discussions with Hamish Ramsay, both of which helped improve this paper.

## 6. REFERENCES

- Bunkers, M. J., B. A. Klimowski, J. W. Zeitler, R. L. Thompson, and M. L. Weisman, 2000: Predicting supercell motion using a new hodograph technique. *Wea. Forecasting*, **15**, 61–79.
- Davies-Jones, R., 2002: Linear and nonlinear propagation of supercell storms. *J. Atmos. Sci.*, **59**, 3178–3205.
- Droegemeier, K. K., S. M. Lazarus, and R. Davies-Jones, 1993: The influence of helicity on numerically simulated convective storms. *Mon. Wea. Rev.*, **121**, 2005–2029.
- Hart, J. A., and W. D. Korotky, 1991: *The SHARP Workstation - v1.50. A Skew T/Hodograph Analysis and Research Program for the IBM and Compatible PC. User's Manual*. NOAA/NWS Forecast Office, Charleston, WV, 62 pp. [Available from NOAA Central Library, 1315 East-West Highway, Silver Spring, MD 20910.]
- Kirkpatrick, J. C., E. W. McCaul Jr., and C. Cohen, 2006: The motion of simulated convective storms as a function of basic environmental parameters. *Mon. Wea. Rev.*, provisionally accepted.
- Klimowski, B. A., and M. J. Bunkers, 2002: Comments on "Satellite observations of a severe supercell thunderstorm on 24 July 2000 made during the GOES-11 science test." *Wea. Forecasting*, **17**, 1111–1117.
- Lilly, D. K., 1982: The development and maintenance of rotation in convective storms. *Intense Atmospheric Vortices*, L. Bengtsson and J. Lighthill, Eds., Springer-Verlag, 149–160.
- Livezey, R. E., 1999: Field intercomparison. *Analysis of Climate Variability: Applications of Statistical Techniques*. H. von Storch and A. Navarra, Eds., Springer-Verlag, 161–178.
- Ramsay, H. A., and C. A. Doswell III, 2005: A sensitivity study of hodograph-based methods for estimating supercell motion. *Wea. Forecasting*, **20**, 954–970.
- Rasmussen, E. N., and D. O. Blanchard, 1998: A baseline climatology of sounding-derived supercell and tornado forecast parameters. *Wea. Forecasting*, **13**, 1148–1164.
- Weisman, M. L., and J. B. Klemp, 1984: The structure and classification of numerically simulated convective storms in directionally varying wind shears. *Mon. Wea. Rev.*, **112**, 2479–2498.
- \_\_\_\_\_, and R. Rotunno, 2000: The use of vertical wind shear versus helicity in interpreting supercell dynamics. *J. Atmos. Sci.*, **57**, 1452–1472.
- Zeitler, J. W., and M. J. Bunkers, 2005: Operational forecasting of supercell motion: Review and case studies using multiple datasets. *Natl. Wea. Dig.*, **29** (1), 81–97.